Pergamon

Geochimica et Cosmochimica Acta, Vol. 58, No. 2, pp. 595–611, 1994

0016-7037/94 $6.00 + .00

The albite-water system: Part I. The kinetics of dissolution as a function of pH at 100, 200, and 300°C

ROLAND HELLMANN

Laboratoire de Géochimie, U.R.A. 067 du C.N.R.S., Université Paul Sabatier 38, rue des Trente-Six Ponts, 31400 Toulouse, France
and Laboratoire de Géophysique Interne et Tectonophysique, U.R.A. 733 du C.N.R.S., Université Joseph Fourier I.R.I.G.M.
BP 53X, 38041 Grenoble cedex, France

(*Received February* 2, 1993; *accepted in revised form August* 16, 1993)

Abstract—Albite feldspar was hydrolyzed at 100, 200, and 300°C in solutions at pH values ranging from 1.4 to 10.3. The dissolution experiments were carried out in a single-pass tubular flow system. Rates were determined both by the mass loss of the sample and from the reactor output concentration of released Si. All of the measured rates represent limiting rates since the experiments were run at conditions far from equilibrium with respect to albite saturation. The only secondary phase to form was boehmite, precipitation of which mostly occurred under acid conditions. The dissolution rate curves displayed a U-shaped relationship with pH, as evidenced by a decrease in the rates with increasing pH in the acid region, a neutral pH region marked by no pH dependence, and a basic pH region where the rates increased with increasing pH. For any given temperature, the absolute values of the slopes (n) of the log rate vs. pH curves were approximately equal in the acid and basic pH regions. The absolute values of n increased from 0.2 to 0.6 in both the acid and basic pH regions as the temperature increased from 100 to 300°C. The calculated energies of activation were 89, 69, and 85 kJ/mol in the acid, neutral, and basic pH regions, respectively. These values reflect the greater dependence of the rates on temperature in the acid and basic pH ranges in comparison to the neutral pH range. The results from this study have been compared to a few published studies in the literature concerning the hydrolysis of albite and other feldspars at 100°C and higher temperatures. A comparison of the rates revealed that the differences in rates are potentially dependent on the design of the experiments. Even after taking into account experimental uncertainties, it appears that static hydrolysis experiments almost always produce measured rates that are lower than those obtained in flow systems. This may be explained by the precipitation of secondary phases and/or chemical affinity considerations.

INTRODUCTION

THE HYDROLYSIS OF MINERALS is of primary importance in understanding the evolution and behavior of water-rock systems. The domain of water-rock interactions spans a wide range of geological environments: chemical and physical weathering reactions on the Earth's surface, diagenetic alteration of sediments in sedimentary basins and subduction zones, hydrothermal circulation in the upper to middle crust, metasomatic reactions associated with regional metamorphism; these are just a few examples where water-rock interactions control the dissolution and precipitation behavior of minerals, the chemical composition of the fluids in contact with the minerals, and the mass transport of dissolved constituents.

In order to understand the complex nature of how rocks behave in contact with water, the problem must first be approached with the study of mineral hydrolysis reactions. Only when the hydrolysis behavior of the individual mineralogical components of rocks is understood can one hope for the development of realistic theories and models of large scale water-rock interactions. Since feldspars are the most common mineralogical constituent of the upper crust (ANDERSON, 1989), their hydrolysis behavior is of significant geochemical interest.

The study of feldspar dissolution dates back to the last century with the studies of DAUBRÉE (1867). Experiments of TAMM (1930) and CORRENS and VON ENGELHARDT (1938) were representative of the first modern-day approach to feldspar hydrolysis, thereby setting the stage for the more-recent evolution of interest in feldspar hydrolysis. Over the intervening years, quite a few studies have been devoted to the dissolution behavior of feldspars at room temperature; perhaps no other mineral has been so extensively studied in the field of geochemical dissolution kinetics. Some of the more recent studies at room temperature are those of WOLLAST (1967), BUSENBERG and CLEMENCY (1976), HOLDREN and BERNER (1979), (a more complete compendium of pre-1982 published studies is given in AAGAARD and HELGESON, 1982; for an interpretation of some of the pre-1984 literature data, see HELEGESON et al., 1984), CHOU and WOLLAST (1984, 1985), HOLDREN and SPEYER (1985), KNAUSS and WOLERY (1986), MAST and DREVER (1987), AMRHEIN and SUAREZ (1988), SCHWEDA (1990), CASEY et al. (1989, 1991). At temperatures up to 100°C, the number of dissolution rate studies is more limited: KNAUSS and WOLERY (1986), ROSE (1991), BURCH et al. (1993). There have also been a number of experimental studies on the influence of acetic and oxalic acids on feldspar dissolution at 100°C, such as those of HUANG and LONGO (1992) and FRANKLIN et al. (unpubl. results, pers. commun. HAJASH, 1993), (see also references listed in the former study). At temperatures above 100°C, experimental work has been published by MOREY and CHEN (1955), MOREY and FOURNIER (1961), LAGACHE

(1965, 1976), TSUZUKI and SUZUKI (1980), HELLMANN (1989), HELLMANN et al. (1989, 1990), RAFAL'SKIY et al. (1990), RAFAL'SKIY and PRISYAGINA (1991).

Despite the fact that so much experimental attention has been given to the study of feldspar hydrolysis, published dissolution rates measured at 25°C have differed by up to an order of magnitude. This is in part due to the long times needed to achieve steady-state reaction conditions at low temperatures. In addition, feldspar dissolution can be very complicated due to the incongruent release of elements as a function of pH, as well as the surface precipitation of secondary, supersaturated phases. At elevated temperatures, the fundamental problems of investigating the dissolution behavior of feldspars are exacerbated by the problems associated with the rapid precipitation of secondary phases, making the extrapolation of rate constants from the measured dissolution rates very difficult. The only factor in favor of the experimentalist working at higher temperatures is the fact that steady-state conditions are approached several orders of magnitude faster than at room temperature.

The paucity of high temperature ($\geq$100°C) kinetic data was the main motivating factor for studying the hydrolysis of feldspar under hydrothermal conditions. The specific goals of this study were the determination of dissolution rates, rate constants, pH dependencies, and activation energies based on the hydrolysis of albite feldspar at 100, 200, and 300°C over a wide range of pH values. The extrapolated rate constants from this study, combined with the calculated energies of activation and pH dependencies, will complement low temperature data currently available, but which are quite often lacking in agreement. These are the types of kinetic data necessary for better constraining the quantitative aspects of existing theories and models of water-rock interactions at elevated temperatures and pressures. Another important goal of this study was a detailed comparison of data from previously published studies; this provided a means for analyzing the influence of experimental design on the measurement of kinetic data. Even though the immediate goal of this study was not a comprehensive treatment of reaction mechanisms, macroscopic kinetic information of this kind is very useful for elucidating the mechanisms of hydrolysis reactions, when coupled with microscopic-scale data derived from the application of various spectroscopic and microscopic techniques. In a series of upcoming companion papers, several additional subjects will be treated in detail: an analysis of the release rates of Na, Al, and Si as a function of time, the surface chemistry of albite after hydrolysis, and a summary study that will address the mechanisms of dissolution.

EXPERIMENTAL METHODS

Albite feldspar was chosen for the considered dissolution experiments since it has an endmember composition and it is also very well characterized in the mineralogical literature (for an overview, see SMITH and BROWN, 1988). Albite from the Amelia Court House pegmatite (Virginia, USA), purchased from Ward's Scientific Est., was used in these experiments in as is condition. The endmember chemical composition ($NaAlSi_3O_8$) of this pure albite was confirmed by microprobe analyses (Table 1). The degree of ordering of structurally low albite from Amelia can be calculated from the detailed crystallographic data given in HARLOW and BROWN (1980); references to ordering can also be found in SMITH and BROWN (1990). For each experiment, a 1 cm × 1 cm sample was cleaved from the parent sample and then ultrasonically cleaned in ethanol for 15 min. The main advantage of using large samples is the avoidance of sample preparation artifacts induced by grinding (see EGGLESTON et al., 1989). Grinding of samples is a well-known cause for both enhanced surface strain and the creation of surface fines. Since it was assumed that the sample surfaces were not additionally strained to any significant degree during cleavage, annealing was deemed unnecessary. In addition, large samples more easily allow the use of certain surface spectroscopic and microscopic techniques.

Table 1: Microprobe analyses of the low albite from Amelia used in this study*

oxide	wght. %	1σ
SiO_2	67.19	0.43
Al_2O_3	21.25	0.20
Fe_2O_3	0.04	0.09
MgO	0.0	-
MnO	0.02	0.06
CaO	0.0	-
Na_2O	12.21	0.16
K_2O	0.0	-
Sum	100.71	

*based on 10 analyses of 3 separate areas

Surface areas were measured by a multipoint static gas adsorption technique (using Kr as the adsorbate), based on the theory presented by BRUNAUER et al. (1938). Due to the low surface area of the samples, the surface area determinations were close to the analytical limit of the technique, and were estimated to be accurate to within 20–30%. The adopted surface area value for the cleavage fragments was 0.013 m^2/g. Repeated measurements of a surface area standard yielded values within 15–20% of the stated surface area. Geometrically measured surface areas were lower by a factor of 1.5. No attempt was made to measure post-hydrolysis surface areas.

The experiments were run using a one-pass, tubular flow-through circulation apparatus. A schematic diagram of the apparatus is shown in Fig. 1. All wetted parts, with the exception of the back-pressure regulator (316 stainless steel), were constructed of high grade titanium in order to limit the effects of corrosion. Inflowing solutions were pumped by a HPLC pump at rates varying from 0.1 to 3.0 mL/min. Solutions were preheated (to a maximum of 180°C) before contacting the sample, which resided midway in a tubular reactor. The horizontally-positioned reactor was heated independently by a tubular furnace. The temperature was monitored by two chromel-alumel thermocouples located in wells positioned longitudinally within the reactor walls. The system pressure was maintained at a constant value of 170 bars by the back-pressure regulator. The aqueous effluent was sampled at the downstream end of the regulator.

The internal volumes of the tubular reactors used ranged from 4 to 7 cm^3. If one takes an average reactor volume of 5.5 cm^3, the corresponding fluid residence times would range from 2–55 min. Since the sample took up only a small part of the total reactor volume, the contact time of fluid with a given sample was considerably less than the overall residence time. If one considers a reactor volume element corresponding to 1 cm length, this changes the range of effective contact times in the experiments to 0.1–3.0 min.

In a tubular (one-pass) flow-through reactor, a given packet of solution contacts the sample only once. The pH of the incoming solution remains the same over time for any given run (in contrast to a batch reactor, where the pH continually changes, unless the solution is buffered). This is one reason why ionic strength-pH buffers were not added to the input solutions. A second reason for the omission of buffers is that organic ligands and salts can potentially affect the kinetics of dissolution. Several studies in the past have noted slight differences in dissolution rates as a function of the concentration and chemical composition of the buffer used (GRANDSTAFF, 1986; CARROLL-WEBB and WALTHER, 1988; ROSE, 1991). The effect of

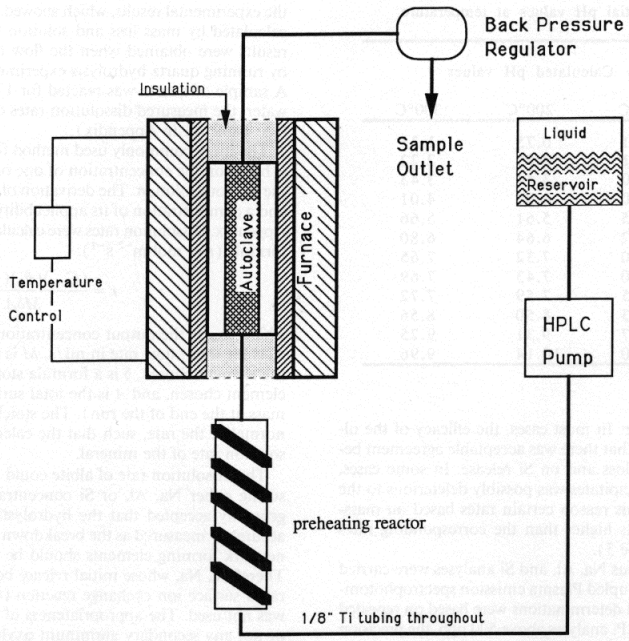

FIG. 1. Schematic diagram of the one-pass tubular flow system used. All wetted parts, including tubing, were of high-grade titanium, in order to limit the effects of corrosion; only the back-pressure regulator was constructed of 316 stainless steel. Solutions were pumped with a HPLC pump into a preheating autoclave, where solutions were preheated to a maximum of 180°C. The sample was located midway in the horizontally positioned tubular reactor, which resided in an independently temperature controlled furnace. The system pressure was always maintained at 170 bars by the back-pressure regulator. The aqueous effluent was sampled at the outflow end of the back-pressure regulator. Diagram modified from HELLMANN et al. (1990).

competing cations on the dissolution rate of quartz was recently demonstrated in a study by DOVE and CRERAR (1990); their results showed that small concentrations (up to 0.05 m) of NaCl and KCl increased the rate of dissolution by up to 1.5 orders of magnitude with respect to pure water.

The lack of buffers in this study implied that the ionic strength of the input solutions was solely a function of the concentration of HCl or KOH used for adjusting the solution pH in the acid and basic pH regions, respectively. Therefore, at acid pH, the positive ion contribution to the total ionic strength was due solely to the $[H^+]$, and conversely, at basic pH, the $[OH^-]$ was the sole negative ion contribution to the total ionic strength. According to the results of BLUM and LASAGA (1988), there is a direct relationship between the adsorption of H^+ and OH^- and rates of albite dissolution. This has important implications for this study, since the ions which determined the ionic strength of the solutions probably controlled the kinetics of dissolution, as well.

Stock solutions for the experiments were prepared with eighteen MΩ deionized water and stored in polyethylene containers. No attempt was made to exclude CO_2 from the solutions. Solutions were pH-adjusted with HCl or KOH (both analytical grade). Stock solutions were pH-adjusted and left open to the atmosphere for at least 24 hours; before each experiment was run solution pH values were readjusted as necessary. Solution pH remained constant to within ±0.05 units during the duration of any given experiment; the one exception was in the neutral to slightly basic pH 7–9 range, where downward pH shifts of up to ≈1.5 units were recorded over 24 hour time spans (probably due to influx of CO_2). As is discussed further on, this shift in pH did not affect the interpretation of the data.

Input solutions in the acid to neutral pH range were assumed to be saturated with respect to atmospheric CO_2, based on measured pH values of 5.7 for input solutions of plain deionized water left exposed to the atmosphere. Stock solutions in the basic pH range were not saturated with atmospheric CO_2, as shown by carbonate equilibria calculations using the geochemical computer code package EQ3/6 (WOLERY, 1983; WOLERY and DAVELER, 1990). The f_{CO_2} of the alkaline solutions was calculated by adjusting the total $[CO_2]_{aq}$ until the solution was electrically neutral, based on the fixed concentrations of H^+ and K^+ which were measured in the input solutions. pH at experimental temperature was also calculated using EQ3/6. For acidic solutions, the difference in calculated pH values for a given solution from 25° to 300°C was minor, never exceeding several tenths of a pH unit. The influence of both temperature and $[CO_2]_{aq}$ on the pH of neutral to alkaline solutions was much greater, such that in-situ pH values at 300°C were on average 2–3 pH units lower than the corresponding solution pH values at 25°C. The calculated in-situ pH values for the experiments are listed in Table 2.

The majority of the experimental runs lasted approximately 24 h. Some high-temperature runs (300°C) were significantly shorter or longer (up to 248 h). Samples run at 100°C were hydrolyzed from a minimum of 24 h to a maximum of 57 h. In each case, a sample of known mass was introduced into the reactor, the temperature of the reactor was raised to the desired value, and then the solution was pumped through the system. Aqueous samples of the effluent (output) stream were taken frequently (several times per hour, tapering off to once every few hours towards the end of a run). The pH of effluent samples was measured at 25°C; there were no measurable differences between the input and output pH. Aqueous samples were acidified with concentrated analytical-grade HCl and subsequently analyzed for Na, Al, and Si. The recovered albite samples were rinsed with water and allowed to dry before their masses were determined. Secondary precipitates (boehmite), if present, were removed by ultrasonic

Table 2: Calculated initial pH values at temperature.

pH meas. 25°C	Calculated pH values		
	100°C	200°C	300°C
0.7	0.71	0.75	1.35
2.0	2.01	2.02	2.22
3.4	3.40	3.41	3.43
4.0	4.00	4.00	4.01
5.7	5.65	5.61	5.66
6.8	6.72	6.64	6.80
8.7	7.60	7.32	7.65
9.6	8.10	7.43	7.69
10.0	8.45	7.59	7.72
11.0	9.43	8.50	8.56
12.0	10.27	9.31	9.25
13.1	11.20	10.14	9.96

treatment in deionized water. In most cases, the efficacy of the ultrasonic treatment was such that there was acceptable agreement between rates based on mass loss and on Si release. In some cases, however, the removal of precipitates was possibly deleterious to the underlying albite, and for this reason certain rates based on mass-loss were up to 0.5 log units higher than the corresponding rates based on Si release (see Table 3).

The majority of the aqueous Na, Al, and Si analyses were carried out by I.C.P. (Inductively Coupled Plasma emission spectrophotometry). Accuracy and precision determinations were based on repeated analyses of standards. For I.C.P. analyses above 500 ppb, the precision and accuracy were approximately 10%; below 500 ppb this figure increased to 15–20%. While the majority of Na analyses were done by I.C.P., a few samples with concentrations above 1 ppm were also performed by flame emission spectrophotometry; the analytical precision and accuracy were about equal to that of I.C.P. Aluminum analyses below 50 ppb were performed using standard atomic absorption furnace procedures; analytical precision and accuracy were estimated to be 20%. Silicon was analyzed colorimetrically at concentrations below 1 ppm using an automated Si analyzer; analytical precision and accuracy were estimated to be in the range of 5–10%. At very low concentrations (<100 ppb), Si was analyzed colorimetrically using the molybdate blue method (STRICKLAND and PARSONS, 1972); the estimated precision and accuracy were the same as with the Si autoanalyzer. This method allows for the determination of Si down to 5 ppb.

EXPERIMENTAL CALCULATIONS

Dissolution Rate

The rates of dissolution of albite feldspar were calculated both from the mass loss of the sample and from the concentration of released Si in the solution. The large size of each sample facilitated the determination of rates by mass loss. The following formula was used to calculate the dissolution rate r (mol m^{-2} s^{-1}):

$$r = \frac{\Delta m}{(M)(t)(A)}, \tag{1}$$

where Δm is the difference between the initial and final mass in grams, M is the formula weight (albite = 262.219 g/mol), t is the experimental time in seconds, and A is the total surface area in m^2. The mass-loss rate calculations were based on a surface area calculated from the average of the initial and final mass of the sample. This assumes that the surface area is a linear function of the sample mass; thus, the surface area used for each calculation is proportional to an intermediate value of the sample mass during the run. This assumption of a linear dependence is, strictly speaking, not accurate, since it neglects the formation of etch pits and other surface features. Nonetheless, at elevated temperatures, the rapid rate of hydrolysis and the concomitant decrease in mass seemed to counteract the effect of increasing surface area due to the appearance of surface dissolution features. The validity of this assumption was generally supported by the experimental results, which showed close agreement between rates calculated by mass loss and solution concentrations of Si. Similar results were obtained when the flow reactor system was calibrated by running quartz hydrolysis experiments at elevated temperatures. A sample of quartz was reacted for 17 days at 300°C in deionized water, the measured dissolution rates differed only by 0.03 log units (see Table A1 in Appendix).

The more commonly used method for calculating dissolution rates is based on the concentration of one or more elements released into the aqueous solution. The derivation of the rate formula shown below and a demonstration of its applicability to this study are given in the Appendix. Dissolution rates were calculated according to the following formula (r in mol m^{-2} s^{-1}):

$$r = \frac{(C_{out})(\vartheta_0)(10^{-6})}{M\delta A}, \tag{2}$$

where C_{out} is the output concentration of a given element in mg/l, ϑ_0 is the input flow rate in ml/s, M is the atomic weight (g/mol) of the element chosen, δ is a formula stoichiometric coefficient for the element chosen, and A is the total surface area in m^2 (based on the mass at the end of the run). The stoichiometric coefficient serves to normalize the rate, such that the calculated rate represents the dissolution rate of the mineral.

The dissolution rate of albite could have been calculated by measuring either Na, Al, or Si concentrations in solution. Since it is generally accepted that the hydrolysis of silicate minerals is most accurately measured as the breakdown of the network structure, only network forming elements should be used for rate determinations. Therefore, Na, whose initial release behavior can be described by a rapid surface ion exchange reaction (CHOU and WOLLAST, 1985), was not used. The appropriateness of using Al depends on whether or not any secondary aluminum oxyhydroxide phases form due to precipitation reactions. The overall release rate of Al can be represented by the following expression:

$$\text{rate}_{\text{Al (overall)}} = \text{rate}_{\text{Al release}} - \text{rate}_{\text{Al precipitation}}. \tag{3}$$

In the present experiments, boehmite (AlO(OH)) commonly precipitated, predominantly at acid pH, as a surface rind on the dissolving mineral sample. A recent study (HELLMANN et al., 1989) showed that boehmite rinds can completely armor an albite surface during high temperature, low pH hydrolysis. SEM images of samples after hydrolysis, which had been cleaved-apart, revealed the existence of 0.5 mm-thick boehmite rinds (see Figs. 8 and 9 of the aforementioned study). Due to the high porosity associated with the bladed aggregates of boehmite crystals making up this rind, the rind was postulated not to act as a diffusional barrier to the release of Si. In the present study, the experimental run times were shorter than in the experiments by HELLMANN et al. (1989), such that the boehmite rinds were significantly less important in thickness.

The obvious difficulty of measuring precipitation kinetics under the considered experimental conditions necessitated using Si release rates as the indicator of the overall rate of dissolution of albite. Since Si was used for the rate calculations, $\delta = 3$ was used as the stoichiometric normalization coefficient in Eqn. 2. The presence of boehmite rinds on samples run at high temperatures under acid conditions apparently did not affect the release rate of Si. This was substantiated by the constant release rates of Si with time and by the linear trend of the activation energy plot for acid pH conditions, shown in Fig. 5a (i.e., log rate constant vs. inverse temperature). If the rinds had acted as a diffusional barrier, or had provided sites for adsorption, then the calculated rate constants would have increasingly diverged from a linear relationship with increasing temperature. There is an additional argument that Si would not be subject to large-scale adsorption on boehmite surfaces: Si under acid conditions occurs as H_4SiO_4; it is unlikely that uncharged H_4SiO_4 groups would be adsorbed to positively-charged boehmite surfaces (pzc of boehmite = 9.2; ALWITT, 1972).

Attainment of Steady State

All of the kinetic data that are reported in this study represent steady-state rates; these have also been referred to as limiting rates (KNAUSS and WOLERY, 1986) or plateau rates (NAGY and LASAGA, 1992) in previous kinetics studies. This means that the rates were

measured beyond the initial, transient period of hydrolysis that is characterized by the dissolution of surface fines and any preexisting strained surface layer. The formation of leached layers on hydrolyzed feldspar surfaces (CASEY et al., 1989; HELLMANN et al., 1990) implies a potential additional constraint, depending on which element is chosen as the indicator for the overall dissolution rate of the mineral. Steady-state conditions of release mandate that the preferential leaching of elements attains a constant value and, therefore, a constant depth. Once steady-state conditions are reached, the aqueous concentrations of all elements should not change with time, and the stoichiometric ratios between preferentially released elements and a conservative (not preferentially released) element in solution are equal to the equivalent ratio in the solid. In the case of the present experiments, Na and Al were almost always preferentially released, and Si behaved conservatively. For nearly all conditions of hydrolysis, the preferential release of Na and Al with respect to Si was demonstrated by following the release rates of all three elements with time. Therefore, even though Al frequently precipitated as a secondary aluminous phase under acid conditions (as indicated by negative Al/Si relative release ratios; see Table 3), the very initial Al release rates were higher than those of Si. Even though more details cannot be given here, the evolution of the release rates with time forms the basis of an upcoming companion paper.

The only important criterion for the calculation of the dissolution rates was that the Si release rates attained a steady state, and not whether the Na and Al release rates were indicative of their respective leached layers having reached a constant depth (this holds especially true for the 100°C results). This idea can be clarified by an examination of the results for samples Q and Q′ (rehydrolysis of Q), as shown in Fig. 2 and Table 3. One can note that their final rates of Si release at 100°C are the same (within the experimental uncertainty), even though their Al/Si and Na/Si relative release ratios are markedly different.

In this study, dissolution rates for experiments run at 100° and 200°C were based on hydrolysis times of at least 24 h. In some cases, experiments were run for much longer periods of time, up to a maximum of 86 h. To ensure that samples run at 100°C had reached steady state, several samples were re-run several weeks later to ensure that there was no change in the calculated dissolution rates. The results showed that 24 hours was sufficiently long for the attainment of steady-state rates at 100°C. Steady-state rates were obtainable much more rapidly at higher temperatures, such that at 300°C, 5 hours was sufficient.

Figure 2 shows the time evolution of dissolution rates, based on Si release, of four samples run at 100°C. The mass loss of these samples was either not measurable (<0.1 mg) or insignificant, such that the surface areas were considered to be constant. The time evolution of the rates was strongly dependent on pH in terms of the magnitude of the initial rate and the time required to attain steady state. At neutral pH, one sample was rehydrolyzed (Q and Q′), and as is shown in Fig. 2, the only important difference in their behavior was a lower initial rate in Q′ (the sample which was re-run). The most important result to be noted is the fact that the rate of Q after 24 hours matches that of Q′ after 62 hours of rehydrolysis.

In summary, Fig. 2 demonstrates that 24 hours were sufficient for hydrolysis reactions at 100°C and neutral pH to reach steady-state rates, and at acid and basic pH the time to reach steady state was even shorter. At 200° and 300°C, steady-state rates were attained over time periods significantly shorter than 24 hours for all pH ranges. The strong dependence of the time to reach steady state on solution pH has also been noted by KNAUSS and WOLERY (1986); experiments run at 70°C showed that steady-state rates were reached in only 1 day at pH 1.4, whereas 3 days were required at pH 2.1.

EXPERIMENTAL RESULTS AND DISCUSSION

Measured Rates at 100, 200, and 300°C

The measured rates at 100, 200, and 300°C, based directly on the raw experimental data reported in Table 3, are shown in Fig. 3a,b,c, respectively. The plots represent albite disso-

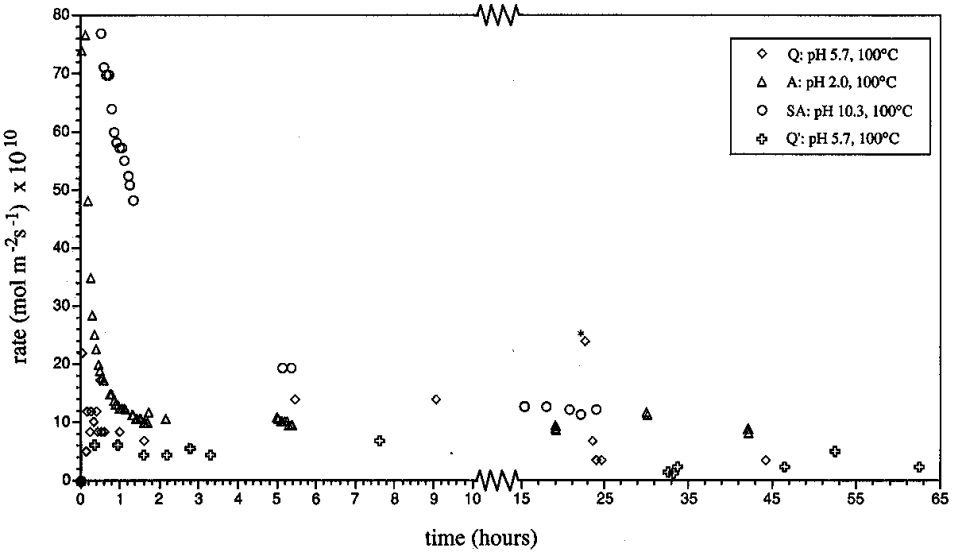

FIG. 2. Attainment of steady state rates-time evolution of dissolution rates at 100°C in pH 2.0, neutral pH 5.7, and pH 10.3 solutions. The attainment of steady-state rates is a strong function of pH. Samples Q and Q′ represent the hydrolysis of the same sample at neutral pH. The important point to note is that the dissolution rate of Q after 24 hours of hydrolysis is the same as the rate of Q′ after 62 hours of rehydrolysis. The sudden rise in the rate of Q (marked by *) was due to a temporary pump failure-steady state dissolution was quickly reestablished. Note that the extrema in the initial rates for samples A and SA are off scale and, therefore, the curves could not be shown in their entirety (t < 1 hour).

Table 3: Results of hydrolysis experiments

Expt. [a]	T (°C)	pH at 25°C	pH_{effec} at T [b]	Time (hours) [c]	log rate [Si] [d]	log rate (mass) [d]	[Si] (ppm) [e]	[Al] (ppm) [e]	[Na] (ppm) [e]	log RRR (Al/Si) [f]	log RRR (Na/Si) [g]	Affinity albite kJ/mol
YB	300	0.7	1.3	19.42	-5.13	-4.50	45.90	14.95	12.42	-0.041	-0.028	91.9
A	100	2.0	2.0	42.15	-9.05	-8.74	0.033	0.017	0.366	0.158	1.585	150.2
A'	100	2.0	2.0	34.40	-9.07	-8.42	0.153	0.073	0.16	0.125	0.559	134.0
B	200	2.0	2.0	47.80	-6.72	-6.65	2.21	0.193	1.033	-0.613	0.21	112.9
C	200	2.0	2.0	86.30	-6.63	-6.76	3.64	0.348	1.33	-0.574	0.103	103.7
L	200	2.0	2.0	23.70	-6.80	-6.90	0.71	0.034	0.40	-0.874	0.291	136.9
D	300	2.0	2.2	24.05		-5.17	0.005	0.046	1.261	1.41	2.942	238.0
E'	300	2.0	2.2	0.08	-5.87		0.677	0.02	2.06	-1.084	1.023	169.8
E''	300	2.0	2.2	2.27	-4.95	-4.65	10.24	0.038	4.155	-1.985	0.148	124.5
G	300	2.0	2.2	0.67	-5.47	-4.49	6.01	0.063	2.09	-1.534	0.081	133.1
M	300	2.0	2.2	24.83	-5.57	-5.54	2.64	0.501	0.87	-0.276	0.058	139.2
RD	300	3.4	3.4	24.25	-6.06	-6.07	4.79	0.025	1.319	-1.837	-0.02	122.6
VB	100	4.0	4.0	24.20	-9.00	-8.77	0.009	0.008	0.154	0.395	1.773	123.4
VB'	100	4.0	4.0	24.03	-9.50		0.013	0.004	0.014	-0.066	0.572	128.8
VB''	100	4.0	4.0	30.37	-9.38	-9.18	0.016	0.007	0.018	0.087	0.591	124.5
VA	200	4.0	4.0	23.42	-7.54	-7.55	0.258	0.002	0.118	-1.665	0.20	136.5
VE	300	4.0	4.0	23.15	-6.36	-6.29	1.875	0.016	0.058	-1.623	0.03	147.3
Q	100	5.7	5.7	44.17	-9.47		0.01	0.205	0.135	1.758	1.67	98.4
Q'	100	5.7	5.7	62.59	-9.62		0.02	0.004	0.019	-0.253	0.518	111.3
P	200	5.7	5.6	24.37	-7.79	-7.65	0.151	0.018	0.098	-0.478	0.352	122.2
O'1	222	5.7	5.6	26.25	-7.27		0.149	0.011	0.020	-0.686	-0.332	140.8
O'2	172	5.7	5.7	24.75	-8.09		0.049	0.052	0.088	0.472	0.794	119.9
O'3	191	5.7	5.6	14.50	-7.61		0.152	0.009	0.030	-0.782	-0.165	125.3
N	300	5.7	5.7	24.08	-6.35	-6.31	2.60	0.854	1.704	-0.038	0.357	87.0
RC	300	5.7	5.7	24.00	-6.44	-6.39	7.06	1.409	2.12	-0.254	0.018	69.3
YA	300	5.7	5.7	248.00	-6.30	-6.39	1.49	0.121	0.483	-0.645	0.051	110.6
YH	300	6.8-6.6	6.8	4.33	-6.13	-5.98	2.82	0.429	0.923	-0.372	0.055	92.0
YF	300	8.7-7.3	7.4	5.42	-6.30	-6.26	2.14	0.534	0.802	-0.157	0.114	95.6
YG	300	9.6-9.2	7.7	10.25	-5.92	-5.95	2.90	0.791	1.081	-0.118	0.111	88.2
TE	100	10.0-9.5	7.7	24.58	-9.35		0.006	0.015	0.47	0.844	2.434	105.0
TE'	100	10.0-8.2	8.2	49.95	-9.77	-9.40	0.023	0.003	0.149	-0.439	1.351	99.6
TA	200	10.0-8.6	7.5	24.00	-7.79	-7.67	0.102	0.043	0.136	0.071	0.665	120.2
TD	300	10.0-9.8	7.7	21.03	-6.03	-5.99	1.268	0.397	0.759	-0.058	0.317	105.1
RE	300	10.9-11.0	8.6	24.00	-6.25	-6.24	6.64	2.13	2.49	-0.048	0.114	70.3
YE	300	11.0-10.9	8.6	6.08	-6.01	-6.00	6.46	1.762	2.88	-0.118	0.189	70.9
SA	100	12.0-12.1	10.3	23.95	-8.92	-8.18	0.027	0.008	3.52*	-0.082	*	112.8
SA'	100	12.0	10.3	57.29	-10.08		0.022	0.01	0.102*	0.103	*	125.0
SF	200	12.0	9.3	24.00	-7.15	-7.01	0.476	0.205	3.85*	0.08	*	102.8
SB	300	12.0	9.2	23.87	-5.97	-6.00	3.53	1.053	4.54*	-0.079	*	88.2
YD	300	12.0-11.9	9.2	13.09	-5.46	-5.59	4.29	1.092	6.72*	-0.148	*	83.4
YC	300	13.1	10.0	7.17	-5.29	-5.34	22.30	5.82	57.30*	-0.138	*	63.7

[a] prime (') denotes rehydrolysis of sample

[b] for pH shift, effective pH corresponding to average $[OH^-]$ over course of experiment

[c] duration of experiment

[d] units of mol $m^{-2}s^{-1}$

[e] output concentration of reactor

[f] log of relative release ratio: log [(Al/Si) solution / (Al/Si) solid]

[g] log of relative release ratio: log [(Na/Si) solution / (Na/Si) solid]

* [Na] too high due to contamination of KOH, therefore RRR not listed

note: expts. E', E'', G were not used in data analysis; SA' also not used (see text)

lution rates (log mol m^{-2} s^{-1}) determined both by mass loss and release of Si to solution. Data from all of the experimental runs are represented, with the exception of run SA' (pH 10.3, 100°C), where an anomalously low dissolution rate, approximately 1.5 log rate units below the mean, was measured. The dissolution rates at 100°C were mostly based on the release of Si, since the mass loss in the individual samples was often too small (<0.1 mg) to be measured. Although the Si concentrations obtained for neutral hydrolysis at 100°C were in the 10–20 ppb range, they were significantly higher

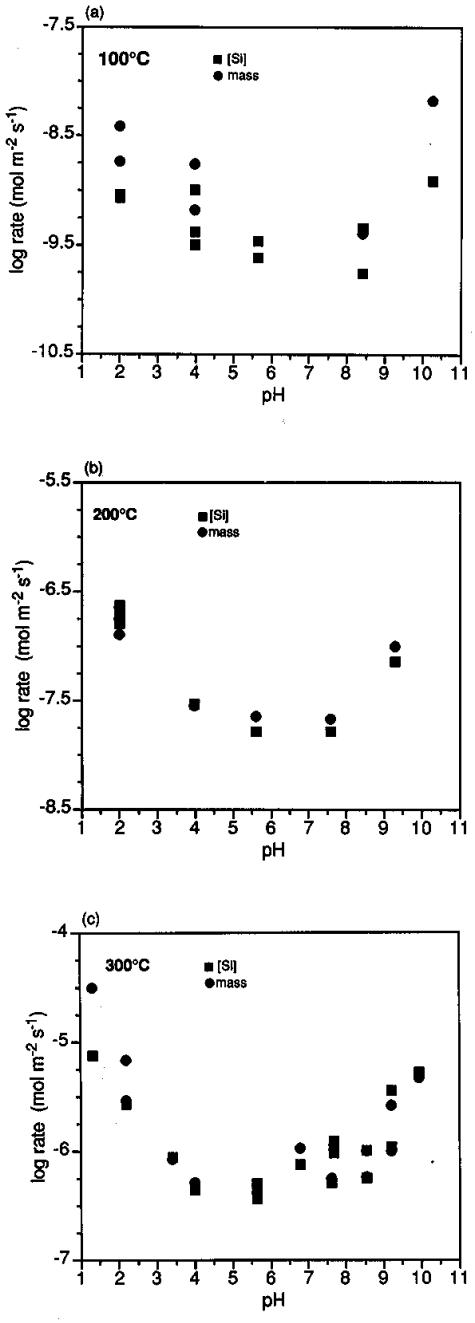

FIG. 3. Dissolution rates at 100° (a), 200° (b), and 300°C (c) as a function of in-situ, initial pH. Note the symmetry of the curves in the acid and basic regions with respect to the neutral pH region. The (absolute) values of the slopes increase from 0.2–0.6 as the temperature is increased from 100° to 300°C. The fact that the rates in the acid and basic regions increase more rapidly with temperature in comparison to the neutral region is reflected in the calculated activation energies.

than the 5 ppb detection limit of the analytical method used. Agreement between the rates determined by the two methods is a strong function of temperature, as can be easily seen by comparing the scatter in the data at 100°C with that at 300°C. The decrease in the scatter of the data at high temperature is probably due to the higher signal-to-noise ratios in the measurements on solutions reacted at higher temperatures. Also, it should be noted (see Table 3) that for a few of the runs in the pH 7–10 range, the pH of the solutions (measured at 25°C) shifted downwards during the course of the experiment (see Table 3, samples YF → TA). The pH drift of these experiments did not alter the results due to the fact that the shifts occurred in the neutral pH range (when the pH was calculated at the in-situ temperature), where the measured rates were independent of pH.

The kinetics of dissolution of any mineral, expressed in terms of a generalized rate law (AAGAARD and HELGESON, 1982), can be written as

$$r_{\text{diss}} = k_+ \prod_i a_i^{-n_{i,j}} f(\Delta G_{\text{diss}}), \tag{4}$$

where r_{diss} is the overall rate of dissolution, k_+ is the rate constant for the forward (dissolution) reaction, a_i is the activity of an ith rate-determining species in the jth reaction, raised to some power n_{ij}, and $f(\Delta G_{\text{diss}})$ is a Gibbs free energy function for the overall dissolution reaction. It has been argued that the form of this generalized rate equation describing a macroscopic process bears a certain similarity (see AAGAARD and HELGESON, 1982) to rate equations written in the framework of transition state theory (TST) (PELZER and WIGNER, 1932; EYRING, 1935; GLASSTONE et al., 1941), where the critical, rate-determining step is based on the breakdown of an activated surface complex. Nonetheless, due to the complexity of silicate hydrolysis reactions, it is important to note that Eqn 4. does not convey information on the mechanisms of elementary reactions, as would be the case for a true TST-rate equation.

The Gibbs free energy function $f(\Delta G_{\text{diss}})$ can take a variety of forms; based on arguments from TST (LASAGA, 1981b; AAGAARD and HELGESON, 1982), it is commonly written as

$$f(\Delta G_{\text{diss}}) = [1 - \exp(\Delta G_{\text{diss}}/RT]^{n*}. \tag{5}$$

The exact form of this equation, as well as the value of n^*, is currently the subject of many dissolution/precipitation studies at, or close to equilibrium conditions (for example, NAGY and LASAGA, 1992). This Gibbs free energy term only influences the overall dissolution rate close to equilibrium conditions. The measure of how far a dissolution reaction is from equilibrium can also be expressed by the chemical affinity of the reaction (A_j), which is defined (DE DONDER and VAN RYSSELBERGHE, 1936) by the following relation:

$$A_j = RT \ln(K_{\text{eq}}/Q), \tag{6}$$

where R is the universal gas constant, T is the absolute temperature, K_{eq} is the equilibrium constant for the hydrolysis reaction, and Q is the reaction quotient for the same reaction. Thus, by definition, the reaction affinity is equal and opposite in sign to the Gibbs free energy of reaction.

Using theoretical TST arguments, AAGAARD and HELGESON (1982) have pointed out that the ΔG_{diss} term in Eqn. 4 does not influence the reaction rate if $A/RT \geq 3$. Experi-

Table 4: Mean dissolution rates and representative uncertainties

Experiment[a]	pH[b]	Temperature (°C)	log mean rate[c]	log ($\mu+2\sigma$, $\mu-2\sigma$)[d]
YB	1.3	300	-4.71	
A, A'	2.0	100	-8.74	-8.34, -9.13
B, C, L	2.0	200	-6.73	-6.58, -6.99
D, M	2.2	300	-5.39	-5.06, -
RD	3.4	300	-6.07	
VB,VB',VB"	4.0	100	-9.09	-8.71, -
VA	4.0	200	-7.55	
VE	4.0	300	-6.33	
Q, Q'	5.7	100	-9.54	
P	5.6	200	-7.71	
N, RC, YA	5.7	300	-6.36	-6.27, -6.48
YH	6.8	300	-6.05	
YF	7.6	300	-6.28	
YG	7.7	300	-5.94	
TE, TE'	8.4	100	-9.47	-9.20,-10.37
TA	7.6	200	-7.73	
TD	7.7	300	-6.01	
RE, YE	8.6	300	-6.11	-5.90, -6.53
SA, SA'	10.3	100	-8.58	
SF	9.3	200	-7.07	
SB, YD	9.2	300	-5.69	-5.35, -
YC	10.0	300	-5.31	

[a] Experiment sample identification. Note that a prime or double prime (' or ") refers to the reutilization of the preceding sample.
[b] In-situ pH (at temperature) at beginning of experiment.
[c] Mean rates based on both [Si] and mass loss, units of mol m^{-2} s^{-1} (see text for details).
[d] Representative (log) uncertainties of mean rates, in some cases log($\mu-2\sigma$) was indeterminable.

mental evidence based on studies of albite dissolution close to equilibrium by BURCH et al. (1993) has shown that the critical affinity value for the albite dissolution reaction at pH 8.8 and 80°C is 37 kJ/mol. The chemical affinity for the dissolution reaction of albite at various temperatures and conditions, based on the output chemistry of the reactor at temperature, were calculated using EQ3/6. The values ranged from 63 to 234 kJ/mol (see Table 3). The measured chemical affinities of reactions in this study were substantially above the theoretically and experimentally determined critical values. Thus, the measured rates were not influenced by the chemical affinity of the reactions. As mentioned earlier, the ability to hydrolyze samples at conditions far from equilibrium is one of the main advantages of flow reactors; this of course is due to the fact that the contact time of a given packet of fluid passing over and interacting with the sample is very small.

Table 4 shows a compilation of the results of the experimental runs, with in-situ pH, temperature, log mean rates, and representative uncertainties (log mean rate $\pm 2\sigma$) listed. Rates were calculated for various combinations of temperature and pH, based on both mass loss and solution composition. Since the rates determined by both of these methods were independent of each other, they were treated as separate rate measurements, and were thus equally weighted when mean rates were determined. The uncertainties in the measured rates vary with both temperature and pH. In general the uncertainties decrease by 0.1–0.2 log rate units as temperatures increase from 100 through 300°C. Uncertainties change similarly as functions of pH (especially at higher temperatures); neutral pH rates have lower uncertainties than do the rates in the acid and basic pH ranges. In terms of the overall uncertainties of the measured rates, it is reasonable to assign a maximum error of 0.4–0.5 log rate units; in most cases, however, the error was in the 0.2–0.3 range. The observed experimental scatter of the data were attributed to experimental errors due to uncertainties in the measurements of temperature, pH, surface area, and the aqueous concentrations of the hydrolysis products. The influence of systematic errors on the uncertainties, which were due to the specific physical and chemical characteristics of the starting materials, or the experimental design, for example, were not taken into account. Uncertainties in the slopes and the intercepts ($\pm 2\sigma$) associated with the linear regression of the rate data were calculated using standard statistical techniques.

Analysis and Comparison with Previously Published Rates

The results reported above have been graphically compared with results published in the literature on albite in Fig. 4, which shows the mean dissolution rates from this study (data from Table 4), with those at 100 and 200°C of LAGACHE (1965, 1976), and those at 225°C of HELLMANN et al. (1990). Albite dissolution rates from several other studies at lower temperatures (ROSE, 1991; KNAUSS and WOLERY, 1986; FRANKLIN et al., unpubl. data; Hajash pers. commun., 1993; CHOU and WOLLAST, 1985) are also shown in Fig. 4. Due to a paucity of experimental dissolution studies of feldspars at temperatures above 100°C, the detailed comparison which follows was not simply restricted to albite, but was extended to include the dissolution rates of other feldspar phases, as well. Thus, not only the studies by LAGACHE (1965, 1976), but those pertaining to other feldspars done by RAFAL'SKIY

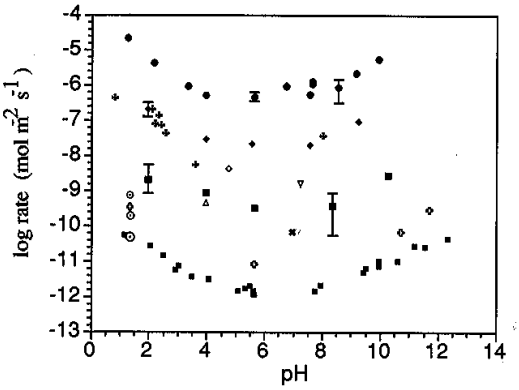

FIG. 4. Comparison of albite dissolution rates from this study (including representative 2σ error bars) with several studies from the literature. The following symbols are used in the figure above: ■ this study 100°C; ◆ this study 200°C; ● this study 300°C; △ LAGACHE (1965) 100°C, $p(CO_2)$ = 6 bars; ▽ LAGACHE (1965) 200°C, $p(CO_2)$ = 0 bar; ◇ LAGACHE (1965) 200°C, $p(CO_2)$ = 6 bars; ✣ HELLMANN et al. (1990) 225°C; ✱ FRANKLIN et al. (unpublished) 100°C; ⊙ ROSE (1991) 90°C; ◎ ROSE (1991) 70°C; ⊙ ROSE (1991) 50°C; ✣ KNAUSS and WOLERY (1986) 70°C; ▪ CHOU and WOLLAST (1984, 1985) 25°C.

et al. (1990) and RAFAL'SKIY and PRISYAGINA (1991), are examined. The retrieved dissolution rates for all types of feldspars, in-situ pH values and representative chemical affinities from the studies mentioned above are given in Table 5.

It should be noted that other studies of feldspar dissolution at elevated temperatures can be found in the literature; three of them are briefly mentioned here. MOREY and CHEN (1955) hydrolyzed Amelia albite in a static system at temperatures up to 350°C, and found that the albite was altered to analcime, boehmite, kaolinite, and dioctahedral micas. The lack of concentration vs. time data precluded the retrieval of reaction rates. Another study, by MOREY and FOURNIER (1961), utilized a semi-static, semi-flow-through system to hydrolyze albite at 295°C. The calculation of reaction rates for their experimental system would have required knowledge of the concentration and pH gradients as a function of the autoclave length (i.e., along the flow axis). In addition, several secondary phases, such as boehmite and paragonite, precipitated over the original albite grains; this would have complicated the retrieval of rates even further. The alteration of labradorite at 230 and 245°C by TSUZUKI and SUZUKI (1980) in static autoclaves also led to the precipitation of several secondary phases. The specific rates and rate laws determined by the authors were based on the premise that these secondary precipitates were responsible for the diffusional inhibition of the hydrolysis reactions.

LAGACHE's (1965, 1976) data

The first set of retrieved rates are based on the pioneering work of LAGACHE (1965, 1976), who hydrolyzed several varieties of feldspar at 100°, 150°, and 200°C in a static (batch reactor) autoclave. In both sets of studies, chemically unbuffered solutions of deionized water were allowed to react for up to 20 days with samples. In all experiments, the solutions were subject to a $p(CO_2)$ of 6 bars (with two exceptions: albite and adularia at 200°C, where $p(CO_2)$ values of 0, 2, 6, and 20 bars were used). Due to the fact that the solutions were static, the fluid compositions continually changed over time due to rising pH, release of elements, and the precipitation of secondary phases. The extrapolated rates of reaction were based on the release of Si (for consistency with this study), as well as on the release of Na (Na and K, for adularia and sanidine). The rate calculations were based on a simple dC/dt analysis of the data from the first 2 days of hydrolysis. The choice of analyzing data after the first 2 days was made in order to limit the effects of both the chemical affinity and the precipitation of secondary phases on the rates of release of Si and Na. For each temperature, the in-situ pH after 2 days of hydrolysis was calculated, using EQ3/6, from the concentrations of released elements and the $p(CO_2)$. With respect to the calculation of rates, the reported geometric surface areas were increased by a factor of 1.5, to bring the surface area measurements in line with those based on gas adsorption (based on BET data of the author for albite grains of approximately the same diameter).

In addition to the rates determined after 2 days of hydrolysis, albite and adularia rates were also calculated for longer periods of hydrolysis, based on stoichiometric Na^+, or Na^+ and K^+, release curves shown in Figs. 16 and 17 of HELGESON et al. (1984). The main difference in the calculations is that the release curves in HELGESON et al. (1984) show a linear regression through data representing longer periods of hydrolysis, and thus the extrapolated rates are lower. Nonetheless, the agreement between both sets of rates was usually very close (see Table 5).

The retrieved log rates for albite at 100 and 200°C are plotted in Fig. 4 as functions of the in-situ pH after 2 days (unless otherwise noted). The calculated log albite rates at 100°C are -9.43_{Si} and -9.35_{Na} (note: throughout this paper, all log rates have units of mol m^{-2} s^{-1}; the subscript refers to the element used for the calculation-if none given, assume Si). As can be seen from Fig. 4, these log rates compare quite well with the 100°C data of this study. The calculated log rates at 200°C and $p(CO_2)$ = 6 and ~0 bars are −8.41, and −8.83, respectively. The difference in reaction rates of 0.4 log units is most probably due to the difference in pH, which is a function of $p(CO_2)$. Nonetheless, the $p(CO_2)$ of the solution may also influence the rate, independently of pH—this should be kept in mind when comparing the results of this study and the rates calculated for Lagache's experiments. With respect to the results at 200°C, the retrieved log rates from Lagache's data are 0.7–1.1 orders of magnitude lower than those from this study. Several other varieties of feldspar, such as adularia, labradorite, and sanidine were hydrolyzed under similar conditions by LAGACHE (1965, 1976). Their rates of dissolution were calculated in a similar manner; the results have been shown in Table 5.

With respect to a comparison only pertaining to albite, one possible explanation for the differences in the dissolution rates is that they are due to differences in chemical affinities. From Table 5, one can note that the albite chemical affinities (based on EQ3/6 calculations) obtained for Lagache's experiments range from approximately 8–25 kJ/mol. For the case of 200°C and $p(CO_2)$ ~0 bar, the chemical affinity of albite was 8.8 kJ/mol; for similar conditions in this study,

Table 5: Retrieved dissolution rates from LAGACHE (1965, 1976), RAFAL'SKIY and PRISYAGINA (1991), RAFAL'SKIY et al.(1990), and HELLMANN et al. (1990).

Mineral	Temp (°C)	$p(CO_2)$ [a] (bar)	Time [b] (hours)	pH [c]	rates r [d,e]	rate r [f]	chemical affinities (kJ/mol)
Albite[1]	100	6	48	3.99	-9.43, -9.35	-9.80	albite (39.42) boehmite (0) pyrophyllite (-0.74) diaspore (-3.83) gibbsite (-5.32) kaolinite (-12.76)
	150	6	48	4.59	-8.55, -8.56	-8.96	albite (31.01) others n.c.
	200	0	48	7.27	-8.83, -9.03	n.c.	albite (8.76) paragonite (-2.88) kaolinite (-3.21)
	200	2	48	5.44	-8.83, -8.64	-8.86	n.c.
	200	6	48	4.80	-8.41, -8.39	-8.53	albite (24.73) gibbsite (-0.83) boehmite (-1.65) diaspore (-4.17) pyrophyllite (-5.11) kaolinite (-11.93)
	200	20	72	4.70	-8.56, -8.35	-8.59	n.c.
Adularia[1]	100	6	48	3.86	-9.72, -9.84	-10.03	n.c.
	150	6	48	4.59	-8.94, -8.95	-9.07	"
	200	6	48	4.70	-8.43, -8.49	-8.79	"
Labradorite[1]	200	6	72	4.88	-8.48, -8.39	n.c.	n.c.
Sanidine[2]	200	6	48	5.35	-8.28, -8.12	n.c.	n.c.
Andesine[3]	150	0	4	7.46	-9.39, -8.86	n.a.	n.c.
	250	0	5	6.83	-8.48, -8.34	"	"
Microcline[4]	150	0	4	3.31	-9.18, -8.85	n.a.	boehmite (0) gibbsite (-2.34) diaspore (-3.17) kaolinite (-7.60)
	250	0	5	6.29	-8.44, -8.30	n.a.	n.c.
Albite[5]	225	0	4.0	0.87	-6.40, n.c.	n.a.	n.c.
	225	0	3.7	2.16	-6.73, n.c.	"	"
	225	0	3.9-9.1	2.26	-7.13, n.c.	"	"
	225	0	3.8-13.7	2.36	-6.91, n.c.	"	"
	225	0	4.1-9.6	2.46	-7.17, n.c.	"	"
	225	0	4.0	2.60	-7.38, n.c.	"	"
	225	0	3.9	3.66	-8.28, n.c.	"	"
	225	0	3.6	8.08	-7.47, n.c.	"	"

[1] data from LAGACHE, 1965
[2] data from LAGACHE, 1976
[3] data from RAFAL'SKIY and PRISYAGINA, 1991
[4] data from RAFAL'SKIY et al., 1990
[5] data from HELLMANN et al., 1990

[a] $p(CO_2)$=0 (=$10^{-3.5}$)
[b] hydrolysis time for rate calc.
[c] in-situ pH at time [b]
[d,e] log (mol m^{-2} s^{-1}), based on [Si],[Na] or [Na+K; adul., sanid.]
[f] calc. from slopes in HELGESON et al.,1984
n.c.= not calculated or listed
n.a. = not applicable

the chemical affinities were in the range from 120–122 kJ/mol. The affinity value determined for Lagache's data was applied in Eqns. 4 and 5, for $n^* = 1$, in order to calculate the affinity correction to the measured rate. The uncorrected log rate was calculated to be −8.83, with an affinity correction the log rate was −8.78. Therefore, it appears that the chemical affinity correction is minor. However, this conclusion would have to be verified, especially when considering that the affinity correction is based not on experimental data, but rather on Eqn. 5, whose exact mathematical form is still the subject of debate (see NAGY and LASAGA, 1992). In addition, it should be noted that a direct comparison with the experimental results from BURCH et al. (1993) should only be done for similar experimental conditions.

The EQ3/6 chemical affinity calculations did, however, reveal perhaps a more important reason for the discrepancies in the rates: the possible presence of several supersaturated phases after just 2 days of hydrolysis (representative chemical affinities of supersaturated phases are also listed in Table 5). In several cases, Al concentrations were probably below the analytical limit of detection and were, therefore, not listed by Lagache. This was most probably due to the precipitation of aluminum oxyhydroxides. For the thermodynamic analysis of those runs, the EQ3/6 calculations were done using Al concentrations that were calculated from the solubility of boehmite. This assumption was reasonable, given that the solutions were supersaturated with respect to boehmite in those runs for which Al concentrations were given, and that LAGACHE (1965) substantiated the presence of boehmite as an alteration product.

The EQ3/6 results in Table 5 show that after two days of albite hydrolysis at 100°C, the solutions became supersaturated with respect to boehmite, pyrophyllite, diaspore, gibbsite, and kaolinite. These phases represent possible sinks for Si and Al. A similar set of phases became supersaturated at higher temperatures. Kaolinite and muscovite, for example,

are two phases which were reportedly identified by X-ray diffraction. Paragonite, a phase predicted to be supersaturated for conditions of 200°C and $p(CO_2)$ ~0 bar, could have been a potential sink for Na, as well. Which secondary phases actually may have precipitated after two days of hydrolysis would have been dependent on the kinetics of precipitation, and not just solely on the saturation indices. The probable reason why the retrieved rate at 100°C matches most closely with this study may be the result of a lack of secondary precipitates, due to the slower kinetics of precipitation at 100 than at 200°C. At higher temperatures, secondary precipitates most probably formed, as evidenced by the changing ratios of Si/Na over time.

In conclusion, the 200°C retrieved rates from LAGACHE (1965) and HELGESON et al. (1984) were generally considerably lower than those determined in this study. The discrepancy in the 200°C rates with those of this study does not come as a surprise, given the fact that the Lagache experiments were carried out in a static system and that several secondary phases probably precipitated, thereby altering the measured Si, and possibly also alkali release rates. These differences prove true a remark made by LAGACHE (1965), "il est évidemment très difficile de comparer directement des résultats obtenus par des techniques si diverses" (i.e., it is very difficult to directly compare results from studies having utilized such different techniques). Nonetheless, despite the differences in experimental design, the retrieved rates at lower temperatures were in relatively close agreement with the results from this study.

Data of RAFAL'SKIY et al. (1990) and RAFAL'SKIY and PRISYAGINA (1991)

The second set of data is from the hydrolysis studies of microcline-perthite ($Na_{0.22}K_{0.75}Al_{1.01}Si_{3.00}O_8$) and andesine ($Ab_{0.65}An_{0.35}$) by RAFAL'SKIY et al. (1990) and RAFAL'SKIY and PRISYAGINA (1991), respectively. As was the case with the experiments of Lagache, the samples were hydrolyzed in a static system. The hydrolysis reactions were carried out at 150° and 250°C in acid solutions (0.001 m HCl solutions), with $p(CO_2)$ apparently set by equilibrium with the atmosphere. For the retrieval of dissolution rates, a specific surface area of 0.15 $m^2\ g^{-1}$ was used; this value being a reasonable estimation in accord with B.E.T. results of the author for feldspar grains in the range of 0.05–0.10 mm.

Using the same strategy as with the interpretation of the Lagache data, rates were determined from dC/dt relations, based on the solution chemistry data for the initial stages of the hydrolysis reactions. In-situ pH's were calculated using EQ3/6; the values calculated were in good agreement with those calculated in the original studies. The extrapolated rates and representative chemical affinities have been tabulated in Table 5. When Al concentration data were not available, chemical affinities were calculated with Al in solution being fixed by the solubility of boehmite. In both studies, elemental release data were available for periods covering the first few hours of hydrolysis. Apparently the hydrolysis reactions were quite rapid since solutions with an initial pH $\approx$ 3.0 became neutral after only 1 hour. Due to the fact that the hydrolysis reactions proceeded extremely fast, the aqueous hydrolysis products rapidly became nonstoichiometric, due mostly to the appearance of secondary phases. For this reason, it was deemed that the most accurate rates could be calculated from dC/dt curves representing the first 4–5 hours of the experiments. Of course, it is recognized that this approach may not have yielded truly accurate rates, since there was no way to determine whether steady-state conditions had been fully achieved before the onset of secondary precipitation reactions.

In regard to the hydrolysis of andesine and microcline, whether based on the release of Si or on alkalis, the retrieved rates are 1–1.5 orders of magnitude lower than the extrapolated values for albite in the present study at 150 and 250°C. In general, the Si-based rates provided the most accurate rates, especially at 150°C. Naturally, some of the discrepancies in the rates are attributable to differences in composition. Nonetheless, as with the LAGACHE (1965, 1976) experiments described above, the rates of dissolution calculated from the experiments of RAFAL'SKIY et al. (1990) and RAFAL'SKIY and PRISYAGINA (1991) were primarily affected by secondary phases. The precipitation of secondary aluminosilicate phases was predicted from mineral stability diagrams in the original studies and was also confirmed by EQ3/6 calculations in the present study. In addition to the formation of secondary precipitates, RAFAL'SKIY and PRISYAGINA (1991) also pointed out that the interpretation of their results must include the reaction for the deanorthitization of andesine to form albite, which can be written as follows:

$$Na_{0.65}Ca_{0.35}Al_{1.35}Si_{2.65}O_8 + 0.7Na^+ + 1.4H_4SiO_4 \rightarrow 1.35NaAlSi_3O_8 + 0.35Ca^{2+} + 2.8H_2O. \quad (7)$$

This reaction consumes released Na, as well as Si. Of course, the albite created is also, in turn, consumed by hydrolysis reactions.

Data of HELLMANN et al. (1990)

The rates reported in HELLMANN et al. (1990) are directly comparable with those of this study, since the hydrolysis experiments were run under almost identical experimental conditions. In this previous study, the albite samples were all hydrolyzed at 225°C, the majority under acid conditions. As can be seen in Fig. 4 and from the tabulated results in Table 5, the mean rates at 225°C in the acid and basic regions are very close to being equal to those of this study at 200°C. However, the rates in the acid region at 225°C should be approximately 0.5 log units higher than the mean rates at 200°C. Given that the uncertainties in the rates are on the order 0.2–0.3 log units, this can only partially explain the discrepancy in the rates. In general terms, the most probable reason for the differences lies with the measurement of very small surface areas associated with such large sample sizes. It should also be noted that at pH 3.7, there is an unacceptably large difference in the rates, since the rate at 225°C is actually lower than that recorded in this study at 200°C. However, the 225°C rate represents only one experimental run over a time period of 3.9 hours, and is most probably not very accurate. In any case, the rates reported in the present study are based on the means of several, individual rates (see Fig. 3b, with individual rates at 200°C); therefore, they should be accorded more statistical significance.

Data of FRANKLIN et al. (unpublished manuscript)

The chief goal of the experiments of FRANKLIN et al. (unpubl. data) was the determination of the effects of carboxylic acids on the rates of dissolution of albite and quartz under diagenetic conditions. A few of their experiments were run at 100°C at neutral pH using distilled water alone. Their experimental system can be described as being a semi-static flow system. Mineral grains were allowed to react with a flowing solution over varying amounts of time; solution sampling was done by taking aliquots of 5–10 ml of the reacted pore fluid, during which the sampled volume was simultaneously replaced by fresh fluid from a syringe pump.

The albite-distilled water experiments were run at flow rates of 8–10 mL/hr, the porosity was 46%, and the experiments lasted from 3–5 hours. The extracted kinetic rates were based on methods which accounted for the change in solute concentration as a function of reactor length and flow rate. Their average retrieved log rate constant at 100°C was −10.2. This value is approximately 0.7 log units slower than that from this study. Their value falls within the lower 2σ bound for the neutral pH, 100°C rate constant from this study (see Fig. 4). The reasons for the difference can be attributed to either experimental uncertainties (due mostly to low surface areas in both this study and theirs), and/or to experimental design and the subsequent interpretation of the data.

Exponents and Dependence of the Rate on pH

A large number of silicate minerals have reaction rates which are a function of pH, such that a typical rate vs. pH curve is U-shaped. The results of this study show the same relationship. To take into account the influence of pH on the rate, rate laws for hydrolysis reactions far from equilibrium, which are based on Eqn. 4, can be written for the three pH regions. For each rate law, k_+ and n are unknowns and can be determined by a linear regression of the log dissolution rate as a function of pH. It is important to note that k_+ can be considered to be a constant for any given temperature and pH region.

In the acid pH range, the dissolution rate r can be expressed in terms of a rate law which is a function of k_+, the forward rate constant, and the activity of H^+ raised to an exponent $-n$

$$r = k_+(a_{H^+})^{-n}. \tag{8}$$

Taking the logarithm of both sides yields

$$\log r = \log k_+ + n(\mathrm{pH}). \tag{9}$$

As is shown later on, at neutral pH there is no discernable relationship between the rate and pH, and, therefore, the rate law can be written as

$$r = k_+(a_{H^+}, a_{OH^-})^{-n=0} \quad \text{or} \quad r = k_+. \tag{10}$$

At basic pH, the rate law can be expressed in terms of the activity of OH^-, such that

$$r = k_+(a_{OH^-})^{n}. \tag{11}$$

Once again, taking the logarithm of both sides and recasting pOH in terms of pH and pK_w (−log of the hydrolysis constant of water), results in the following expression

$$\log r = (\log k_+ - n\,pK_w) + n(\mathrm{pH}). \tag{12}$$

Note that expressing the rate in terms of a_{OH^-} necessitated a sign change for n in Eqn. 11. In both the acid and basic regions, n was determined by plotting log r vs. pH and determining the slope. The slope n is always negative in the acid region and positive in the basic region. It should be noted that the absolute value of the exponent n does not necessarily have the same value in the acid and basic pH regions. In addition to the slope, the y intercept was used to determine the rate constant k_+ for each temperature and pH region. For Eqn. 12 above, values of K_w as a function of temperature were obtained from MARSHALL and FRANCK (1981).

At all three temperatures (100°, 200°, and 300°C) in Figs. 3a,b, and c, the dissolution rate data display a U-shaped relationship as a function of pH. In the acid region, the log rate of dissolution increases linearly with decreasing pH. The neutral region, where rates are pH-independent, spans pH values from ~4–5 to ~7–9. The basic region is defined by the region where the log rate increases linearly with increasing pH. Due to the decrease in the hydrolysis constant of water, K_w, with increasing temperature, the basic region is shifted to lower pH with increasing temperature. The data show that the rate-dependence on pH at acid and basic pH is more or less symmetric about the neutral pH region. There is a change in the rate vs. pH relationship with temperature, as can be noted in the steepening of the slopes at higher temperatures. Within the uncertainties of the data, the slopes remain symmetrical about the neutral pH region as the temperature increases. At 100°C, the exponent $|n|$ in the acid and basic pH regions range equals 0.2 and 0.3, respectively. At 200°C, $|n|$ in both regions equals 0.4, and at 300°C, $|n| = 0.6$ for both regions. Nonetheless, based on the uncertainties in the slopes (Table 6), which range from 0.1 to 0.3, the changes in the dependence of the rate on pH with temperature may not be statistically significant.

Table 6: Rate constants, pH-dependence of rates, and activation energies

Acidic	Rate constant[1]	Exponent	Energy of activation[2]
pH≤ 5	log k_+	$\lvert n_{H^+}\rvert$	Ea
100°C	-8.5 ± 0.5	0.2 ± 0.1	88.9 ±14.6
200°C	-5.9 ± 0.3	0.4 ± 0.1	"
300°C	-4.1 ± 0.5	0.6 ± 0.2	"
Neutral			
5<pH<8.6		n_{H^+}, n_{OH^-}	
100°C	-9.5 ± 0.3	≈ 0	68.8 ± 4.5
200°C	-7.7 ± 0.2	≈ 0	"
300°C	-6.2 ± 0.1	≈ 0	"
Basic			
pH ≥ 8.6		n_{OH^-}	
100°C	-8.3*	0.3*	85.2*
200°C	-6.3 ± 0.7	0.4 ± 0.2	"
300°C	-4.5 ± 0.6	0.6 ± 0.3	"

[1] log mol $m^{-2}s^{-1}$ [2] kJ/mol

uncertainties ($\pm 2\sigma$), * uncert. not determined due to use of only intermediate rate at pH=10.3 (100°C)

Several studies on various feldspar phases have investigated the dependence of dissolution rates on pH. The 25°C data from CHOU and WOLLAST (1984, 1985), which are also shown in Fig. 4, yield an exponent n of -0.5 in the acid region (pH $\leq$ 6) and 0.3 in the basic region (pH $\geq$ 8). For microcline at 25°C, SCHWEDA (1990) found that $n = -0.5$ and 0.7 at acid and basic pH, respectively. The same author determined an exponent of -0.4 for sanidine in the acid region. The 25°C rate data in the basic region in KNAUSS and WOLERY (1986) yielded $n = 0.5$. Several feldspar studies listed in LASAGA (1984) show exponents ranging from -0.5 to -1.0 in the acid range.

At elevated temperatures, the same spread in n can be found. At 70°C, KNAUSS and WOLERY determined that $n = -1.0$ at acid pH, whereas $n = 0.5$ in the basic region. HELGESON et al. (1984), interpreting the data of LAGACHE (1965, 1976), determined an exponent of -1.0 in the acid region, based on the release of Na^+ and K^+, for the hydrolysis of albite, adularia, and sanidine at 100° and 200°C. These results are based, however, on a restricted pH range from 4.8 to 5.5 (for sanidine, see Fig. 9, HELGESON et al., 1984). In addition, it is questionable whether all of the rates used in the extrapolation of n were true limiting rates, as discussed above in the analysis of the Lagache data.

The critical role played by the value of the exponent in the calculation of forward rate constants cannot be overestimated. As an example, for the HELGESON et al. (1984) interpretation of data from LAGACHE et al. (1965) for albite dissolution at 200°C and $p(CO_2) = 6$ bars, the calculated log forward rate constant in the pH-dependent region was determined to be -2.65 mol m^{-2} s^{-1}, which is based on a pH dependence of $n = -1$. Their rate constant (-2.65) is approximately 3.3 log units higher than the rate constant at 200°C determined in this study (-5.9) in the acid pH region. However, if a value of $n = -0.5$ is used (which is reasonable, given that fractional values of n are more preponderant in the literature), their log forward rate constant would decrease by approximately 2.3 log units, to a value of approximately -5.0, which is in much closer agreement to the value determined in this study. This example underlines the drastic effect which a relatively small change in the value of the exponent can have on the value of the forward rate constant. This is also the reason why it was deemed preferable to directly compare the dissolution rates from this study with those in the literature in Fig. 4, rather than comparing the extrapolated rate constants.

Rate Constants

The values of n for the acid region $(a_{H^+})^{-n}$ and the basic region $(a_{OH^-})_n$ were used to derive the forward rate constants k_+, using Eqns. 9 and 12, respectively. In this study, as in the majority of silicate dissolution studies, $n = 0$ in the neutral pH region, which leads to an important simplification: for a given temperature, the dissolution rate r is equal to the forward rate constant k_+. The rate constants k_+ and 2σ uncertainties are listed in Table 6 as a function of pH region and temperature. Because of the symmetric nature of the rate-pH curves about the neutral region, the forward rate constants at acid or basic pH are roughly equal to each other for any given temperature. Nonetheless, even with symmetrical curves, a slight difference in the acid and basic rate constants is to be expected at higher temperatures, because the basic pH region is shifted to lower pH with increasing temperature, which is, of course, a function of the decrease in the hydrolysis constant (K_w) of water.

Energy of Activation

Using the classical Arrhenius relationship,

$$k_+ = Ae^{-E_a/RT}, \tag{13}$$

where A is a pre-exponential frequency factor, E_a is the activation energy, R is the gas constant, and T is the absolute temperature, the activation energies were calculated for the three pH regions. The calculated E_a values (see Table 6) and uncertainties are 88.9 ± 14.6, 68.8 ± 4.5, and 85.2 kJ/mol in the acid, neutral, and basic pH regions, respectively. The lack of an uncertainty in E_a for the basic range follows from the fact that no uncertainty was calculated in the slope n at 100°C (the slope was calculated using only the intermediate rate value at 100°C and pH 10.3; the other two points at that pH far exceeded $\pm 2\sigma$). Figures 5a, b, and c show the regressed data for log k vs. reciprocal temperature from which the slopes were calculated.

Several studies in the literature have yielded data that can be compared with the above energies of activation. To avoid confusion when comparing an energy of activation E_a and an enthalpy of activation $\Delta H^\ddagger$ (where ‡ denotes an activated complex), the following relationship is useful,

$$E_a = RT + \Delta H^\ddagger, \tag{14}$$

(note that both are frequently cited in the literature). The difference in value between the two quantities is generally minor, since $E_a > \Delta H^\ddagger$ by at most ~5–6 kJ/mol for the temperature range of interest. It should also be noted that although this enthalpy of activation is commonly attributed to an activated complex in the literature, it is more realistically representative of an overall enthalpy of activation.

KNAUSS and WOLERY (1986) determined the following activation enthalpies for the dissolution of albite in the acid, neutral, and basic pH regions: 119, 54, and 32 kJ/mol, respectively. The 32 kJ/mol enthalpy of activation for the basic pH range cannot be directly compared to this study without recalculation- the value given is an artifact of a rate law written in a form, where at basic pH, r is dependent on a_{H^+}, rather than a_{OH^-}. Nonetheless, their enthalpy of activation for dissolution in the neutral region is 15 kJ/mol lower than the one in this study, whereas their value for the acid pH region is almost 20 kJ/mol higher. Agreement with the enthalpy of activation for albite dissolution in the acid region given by HELGESON et al. (1984) is surprisingly good, 86 vs. 90 kJ/mol from this study. Based on the slope of the pH-independent curve in Fig. 23a of HELGESON et al. (1984), the enthalpy of activation in the neutral region is 36 kJ/mol. It is important to note, however, that rate constants for several types of feldspars were used to calculate this activation enthalpy. Bearing this in mind, their figure is significantly lower than the 54 kJ/mol value in KNAUSS and WOLERY (1986), as well as the 69 kJ/mol energy of activation from this study. In the

acid pH range, the activation energy for albite of 71 kJ/mol determined by ROSE (1991) is lower than all of the figures given above for the same pH range.

At this point, one can conclude that the agreement in activation energies is not very good either in the acid region nor in the neutral region, while the lack of data makes a comparison for the basic pH region too tenuous. It is difficult to ascertain the reason for the disagreement in the activation energy values, especially at neutral pH, since there is no potential interference from the pH-dependency on the rate constant. From an analysis of the data at neutral pH from this study, as shown in Fig. 5b, the correlation coefficient of the regressed data is fairly good, with $r^2 = 0.9840$. There seems to be no reason to suspect that the 100°C rate constant is too high, since a lower rate constant would have increased the slope of the regressed line even more, thereby yielding an even higher activation energy in the neutral pH range. It is also worth noting that some of the discrepancies in the activation energies may be due to differing enthalpies of H^+ adsorption and desorption at active surface sites. It has been suggested by CASEY and SPOSITO (1992) that these enthalpies of adsorption, which contribute to the energy of activation, change as a function of temperature and pH. In any case, the lack of overall agreement in these energies of activation points to the need for more careful dissolution studies over a wide temperature and pH range.

CONCLUSIONS

The overall goal of this research was an investigation of the hydrolysis behavior of albite in solutions with pH conditions that ranged from very acidic to very basic, and at temperatures ranging from 100° to 300°C. From the measured dissolution rates, rate constants and activation energies were calculated as a function of pH. The main results are summarized below.

1) The rates of hydrolysis were measured at conditions far from equilibrium, therefore, the rates are termed limiting rates. This fact was confirmed by measuring the reactor output concentrations of the released elements and calculating the chemical affinity of albite. For the majority of the experiments, the chemical affinity of albite was in the range of 80–170 kJ/mol. The lowest calculated value was approximately 70 kJ/mol; this is significantly higher than the theoretically and experimentally determined critical values, below which the chemical affinity influences the measured rate of hydrolysis.

2) The rates of hydrolysis show a strong dependence on pH, such that for any given temperature, the extrapolated rate constants in the neutral pH region are 1–2 log rate units less than those in the acid or basic pH regions. The log rate curves show a U-shaped symmetrical dependence on pH, since for any given temperature, the (absolute) values of the slopes are approximately equal for both the acid and basic pH regions. The dependence of the rate on pH under acid and basic pH conditions, respectively, can be expressed as

$$r = k_+(a_{H^+})^{-n}, \quad (15)$$

$$r = k_+(a_{OH^-})^{n}. \quad (16)$$

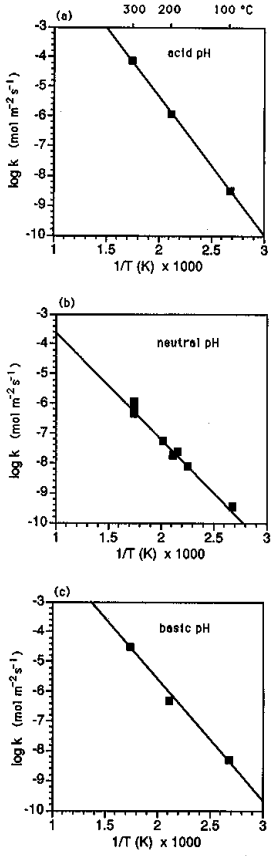

FIG. 5. The rate constants of dissolution as a function of the reciprocal absolute temperature for the acid (a), neutral (b), and basic (c) pH regions. Based on the slopes of the regressed data, the calculated activation energies for the three respective pH regions are 89, 69, and 85 kJ/mol; the uncertainties vary with temperature and are given in Table 6. Note that at neutral pH, 3 additional data were included (samples run at 172–222°C).

For a given temperature the absolute value of the exponent n, within the uncertainty of the calculations, has the same value in both the acid and basic regions. This fact has possible important implications with respect to the mechanisms of dissolution. Thus, even though the aqueous reactant species at acid pH (H_3O^+) and basic pH (OH^-) are different, the formation and breakdown of the surface activated complexes may possibly follow similar paths. The degree of similarity in mechanisms, however, would need to be verified by a detailed analysis of the adsorption and desorption enthalpies associated with hydrolysis.

3) Examination of the family of curves (see Fig. 3) representing the dissolution rate vs. pH reveals that the slopes increase as a function of temperature. This is mirrored in the change of the absolute values of the exponent n (see Eqns.

15 and 16) from 0.2 to 0.6 as the temperature increases from 100° to 300°C. This change in n is reflected in the rate constants, as well. Thus, for a change in temperature from 100° to 300°C, the rate constants in the acid, neutral, and basic regions increase by approximately 4.4, 3.3, and 3.8 orders of magnitude, respectively. Therefore, the rates of reaction at acid and basic pH increase more rapidly as a function of temperature than do the rates at neutral pH. This phenomenon is confirmed by the values for the activation energy, which were determined to be 89, 69, and 85 kJ/mol in the acid, neutral, and basic pH ranges, respectively. The energy of activation values, and their dependence on pH, must be interpreted with care, however. The energy of activation is not solely a function of the energy difference between the reactants and the activated complex, but also may be a function of the energies of adsorption/desorption of aqueous species at activated surface sites (see CASEY and SPOSITO, 1992).

4) In general terms, the energies of activation determined from this study are one important piece of evidence supporting a surface reaction mechanism of dissolution. Most silicates and sparingly soluble oxides have energies of activation in this range, which are several tens of kJ/mol higher than the energies of activation of very soluble minerals, where dissolution is controlled by diffusion at the solid/solution interface (LASAGA, 1981a).

5) One of the most important results of this study is the realization of the potential importance of experimental design on the measured rates of dissolution (the interested reader should also refer to a recent article discussing the extrapolation of reaction rates from batch, mixed flow, and plug flow reactors by RIMSTIDT and NEWCOMB, 1993). A comparison of the results of this study with published studies in the literature reveal that significant differences in rates can be attributed to experimental design alone. Experiments with high solid/solution ratios that are carried out in static reactors often are difficult to interpret, due to the precipitation of secondary phases and to changes in the rate that are due to chemical affinity differences. Even when no apparent reasons can be found for a discrepancy in rates, results of this study, as well as those discussed in reference to quartz in Table A1 of the Appendix, seem to indicate that dissolution rates measured in flow systems can be up to an order of magnitude higher than rates measured in static systems. Nonetheless, flow experiments run under almost identical conditions do not always yield perfectly reproducible rates, either. In addition, the uncertainty in rates also directly influences the extrapolated values of n, which gives the dependence of rate on pH. It is quite obvious that small changes in n lead to drastic changes in values for the rate constant k. Therefore, it is safe to say that the uncertainties in rates are still a big stumbling block to more fully understanding geochemical kinetics.

Acknowledgments—I would like to thank Prof. David A. Crerar of Princeton University for the 18 month loan of one of the flow systems. This study was an extension of kinetics research started as a Ph.D. student with D. A. Crerar- to him this paper is dedicated. The second flow system was carefully machined by C. Lurde at the Université Paul Sabatier, Toulouse. The following people's advice or assistance in the geochemistry lab at Toulouse was appreciated: G. Berger, J.-L. Dandurand, C. Monnin, B. Reynier, J. Schott. The use of an I.C.P. at Societé Bioland in Toulouse is also gratefully acknowledged. Thanks are also due to M. Gugeon for the B.E.T. surface area measurements and C. Davidson (Princeton University) for the microprobe analyses of the Amelia albite. I also thank A. Hajash for making available a copy of an unpublished manuscript. An early critique by E. Silvester, as well as formal reviews by S. A. Carroll, K. G. Knauss, R. Petrovich, and M. F. Hochella, Jr. much improved the original manuscript.

Editorial handling: M. F. Hochella Jr.

REFERENCES

AAGAARD P. and HELGESON H. C. (1982) Thermodynamic and kinetic constraints on reaction rates among minerals and aqueous solutions. I. Theoretical considerations. *Amer. J. Sci.* **282,** 237–285.

ALWITT R. S. (1972) The point of zero charge of pseudoboehmite. *J. Colloid Interf. Sci.* **40,** 195–198.

AMRHEIN C. and SUAREZ D. L. (1988) The use of a surface complexation model to describe the kinetics of ligand-promoted dissolution of anorthite. *Geochim. Cosmochim. Acta* **52,** 2785–2793.

ANDERSON D. L. (1989) *Theory of the Earth.* Blackwell.

BLUM A. and LASAGA A. C. (1988) Role of surface speciation in the low-temperature dissolution of minerals. *Nature* **331,** 431–433.

BRUNAUER S., EMMETT P. H., and TELLER E. (1938) The adsorption of gases in multimolecular layers. *J. Amer. Chem. Soc.* **60,** 309–319.

BURCH T. E., NAGY K. L., and LASAGA A. C. (1993) Free energy dependence of albite dissolution kinetics at 80°C and pH 8.8. *Chem. Geol.* **105,** 137–162.

BUSENBERG E. and CLEMENCY C. V. (1976) The dissolution kinetics of feldspars at 25°C and 1 atm CO_2 partial pressure. *Geochim. Cosmochim. Acta* **40,** 41–49.

CARROL-WEBB S. A. and WALTHER J. V. (1988) A surface reaction model for the pH-dependence of corundum and kaolinite dissolution rates. *Geochim. Cosmochim. Acta* **52,** 2609–2623.

CASEY W. H. and SPOSITO G. (1992) On the temperature dependence of mineral dissolution rates. *Geochim. Cosmochim. Acta* **56,** 3825–3830.

CASEY W. H., WESTRICH H. R., ARNOLD G. W., and BANFIELD J. F. (1989) The surface chemistry of dissolving labradorite feldspar. *Geochim. Cosmochim. Acta* **53,** 821–832.

CASEY W. H., WESTRICH H. R., and HOLDREN G. R. (1991) Dissolution rates of plagioclase at pH = 2 and 3. *Amer. Mineral.* **76,** 211–217.

CHOU L. and WOLLAST R. (1984) Study of the weathering of albite at room temperature and pressure with a fluidized bed reactor. *Geochim. Cosmochim. Acta* **48,** 2205–2218.

CHOU L. and WOLLAST R. (1985) Steady-state kinetics and dissolution mechanisms of albite. *Amer. J. Sci.* **285,** 963–993.

CORRENS C. W. and VON ENGELHARDT W. (1938) Neue Untersuchungen über die Verwitterung des Kalifeldspates. *Chimie der Erde* **12,** 1–22.

DAUBRÉE A. (1867) Expériences sur les décompositions chimiques provoquées par les actions mécaniques dans divers minéraux tels que le feldspath. *C. R. Acad. Sci., Paris* **64,** 339–346.

DE DONDER Th. and VAN RYSSELBERGHE P. (1936) *The Thermodynamic Theory of Affinity.* Stanford Univ. Press.

DOVE P. M. and CRERAR D. A. (1990) Kinetics of quartz dissolution in electrolyte solutions using a hydrothermal mixed flow reactor. *Geochim. Cosmochim. Acta* **54,** 955–969.

EGGLESTON C. M., HOCHELLA M. F., JR., and PARKS G. A. (1989) Sample preparation and aging effects on the dissolution rate and surface composition of diopside. *Geochim. Cosmochim. Acta* **53,** 797–805.

EYRING H. (1935) The activated complex in chemical reactions. *J. Chem. Phys.* **3,** 107–120.

FRANKLIN S. P., HAJASH A. JR., DEWERS T. A., and TIEH T. T. (1993) The role of carboxylic acids in albite and quartz dissolution: An experimental study under diagenetic conditions. *Geochim. Cosmochim. Acta* **58** (in press).

GLASSTONE S., LAIDLER K. J., and EYRING H. (1941) *The Theory of Rate Processes.* McGraw-Hill Book Co.

GRANDSTAFF D. E. (1986) The dissolution of forsteritic olivine from Hawaiian beach sand. In *Rates of chemical weathering of rocks and minerals* (ed. S. M. COLEMAN and D. P. DETHIER), pp. 41–60. Acad. Press.

HARLOW G. E. and BROWN G. E., JR. (1980) Low albite: an X-ray and neutron diffraction study. *Amer. Mineral.* **65,** 986–995.

HELGESON H. C., MURPHY W. H., and AAGAARD P. (1984) Thermodynamic and kinetic constraints on reaction rates among minerals and aqueous solutions. II. Rate constants, effective surface area, and the hydrolysis of feldspar. *Geochim. Cosmochim. Acta* **48,** 2405–2432.

HELLMANN R. (1989) Albite dissolution kinetics at elevated temperatures and pressures. Ph.D. dissertation, Princeton Univ.

HELLMANN R., CRERAR D. A., and ZHANG R. (1989) Albite feldspar hydrolysis to 300°C. In *Reactivity of Solids Proceedings of the 11th Symposium* (ed. M. S. WHITTINGHAM et al.), pp. 314–329. North Holland.

HELLMANN R., EGGLESTON C. M., HOCHELLA M. F., JR., and CRERAR D. A. (1990) The formation of leached layers on albite surfaces during dissolution under hydrothermal conditions. *Geochim. Cosmochim. Acta* **54,** 1267–1281.

HILL C. G., JR. (1977) *An Introduction to Chemical Engineering Kinetics & Reactor Design.* John Wiley & Sons.

HOLDREN G. R., JR. and BERNER R. A. (1979) Mechanism of feldspar weathering-I. Experimental studies. *Geochim. Cosmochim. Acta* **43,** 1161–1171.

HOLDREN G. R., JR. and SPEYER P. M. (1985) pH dependent changes in the rates and stoichiometry of dissolution of an alkali feldspar at room temperature. *Amer. J. Sci.* **285,** 994–1026.

HUANG W.-L. and LONGO J. M. (1992) The effect of organics on feldspar dissolution and the development of secondary porosity. *Chem. Geol.* **98,** 271–292.

KNAUSS K. G. and WOLERY T. J. (1986) Dependence of albite dissolution kinetics on pH and time at 25°C and 70°C. *Geochim. Cosmochim. Acta* **50,** 2481–2497.

LAGACHE M. (1965) Contribution à l'étude de l'altération des feldspaths, dans l'eau, entre 100 et 200°C, sous diverses pressions de CO_2, et application à la synthèse des minéraux argileux. *Bull. Soc. franç. Minér. Crist.* **88,** 223–253.

LAGACHE M. (1976) New data on the kinetics of the dissolution of alkali feldspars at 200°C in CO_2 charged water. *Geochim. Cosmochim. Acta* **40,** 157–161.

LASAGA A. C. (1981a) Rate laws of chemical reactions. In *Kinetics of Geochemical Processes* (ed. A. C. LASAGA and R. J. KIRKPATRICK); *Rev. Mineral.* **8,** 1–68.

LASAGA A. C. (1981b) Transition state theory. In *Kinetics of Geochemical Processes* (ed. A. C. LASAGA and R. J. KIRKPATRICK); *Rev. Mineral.* **8,** 135–169.

LASAGA A. C. (1984) Chemical kinetics of water-rock interactions. *J. Geophys. Res.* **89,** 4009–4025.

MARSHALL W. L. and FRANCK E. U. (1981) Ion product of water substance, 0–1000°C, 1–10000 bars New international formulation and its background. *J. Phys. Chem. Ref. Data* **10,** 295–304.

MAST M. A. and DREVER J. I. (1987) The effect of oxalate on the dissolution rates of oligoclase and tremolite. *Geochim. Cosmochim. Acta* **51,** 2559–2568.

MOREY G. W. and CHEN W. T. (1955) The action of hot water on some feldspars. *Amer. Mineral.* **40,** 996–1000.

MOREY G. W. and FOURNIER R. O. (1961) The decomposition of microcline, albite and nepheline in hot water. *Amer. Mineral.* **46,** 688–699.

NAGY K. L. and LASAGA A. C. (1992) Dissolution and precipitation kinetics of gibbsite at 80°C and pH 3: The dependence on solution saturation state. *Geochim. Cosmochim. Acta* **56,** 3093–3111.

PELZER H. and WIGNER E. (1932) Über die Geschwindigkeitskonstante von Austauschreaktionen. *Z. Phys. Chem.* **B15,** 445–471.

RAFAL'SKIY R. P. and PRISYAGINA N. I. (1991) Reaction of andesine with hot aqueous solutions. *Geochem. Int.* **28,** 72–81.

RAFAL'SKIY R. P., PRISYAGINA N. I., and KONDRUSHIN I. B. (1990) Reaction of microcline-perthite with aqueous solutions at 150 and 250°C. *Geochim. Int.* **27,** 56–66.

RIMSTIDT J. D. and BARNES H. L. (1980) The kinetics of silica-water reactions. *Geochim. Cosmochim. Acta* **44,** 1683–1699.

RIMSTIDT J. D. and NEWCOMB W. D. (1993) Measurement and analysis of rate data: The rate of reaction of ferric iron with pyrite. *Geochim. Cosmochim. Acta* **57,** 1919–1934.

ROSE N. M. (1991) Dissolution rates of prehnite, epidote and albite. *Geochim. Cosmochim. Acta* **55,** 3273–3286.

SCHWEDA P. (1990) Kinetics and mechanisms of alkali feldspar dissolution at low temperatures. Doctoral dissertation, Stockholms Universitets Institution för Geologi och Geokemi.

SMITH J. V. and BROWN W. L. (1988) *Feldspar Minerals 1. Crystal Structures, Physical, Chemical, and Microtextural Properties.* Springer-Verlag.

STRICKLAND J. D. H. and PARSONS T. R. (1972) Determination of reactive silicate. In *A Practical Handbook of Seawater Analysis 167,* pp. 65–70. Fisheries Res. Board Canada.

TAMM V. O. (1930) Experimentelle Studien über die Verwitterung und Tonbildung von Feldspäten. *Chemie der Erde* **4,** 420–430.

TSUZUKI Y. and SUZUKI K. (1980) Experimental study of the alteration process of labradorite in acid hydrothermal solutions. *Geochim. Cosmochim. Acta* **44,** 673–683.

WOLERY T. J. (1983) *EQ3NR, a computer program for geochemical aqueous speciation-solubility calculations: User's guide and documentation. UCRL-53414.* Lawrence Livermore Nat. Lab.

WOLERY T. J. and DAVELER S. A. (1990) *EQ6, a computer program for reaction path modeling of aqueous geochemical systems: User's guide and documentation.* UCRL report. Lawrence Livermore Nat. Lab.

WOLLAST R. (1967) Kinetics of the alteration of K-feldspar in buffered solutions at low temperature. *Geochim. Cosmochim. Acta* **31,** 635–648.

APPENDIX

For a tubular flow reactor operating under steady-state conditions, a material balance can be written on a differential volume element for a dissolution reaction which releases species X,

$$\text{mol}X_{\text{out}} = \text{mol}X_{\text{in}} + \text{mol}X_{\text{by reaction}}. \quad \text{(A1)}$$

In the case of liquid-solid reactions, it is convenient instead to consider a differential element of area. The material balance, when written in terms of molal flow rates (using the formalism in HILL, 1977) becomes:

$$\{F_X + dF_X\}_{\text{out}} = \{F_X\}_{\text{in}} + \{r_X dA_X\}_{\text{by reaction}}, \quad \text{(A2)}$$

where F_X is the molal flow rate of species X (mol s^{-1}), r_x is the rate of release of X (mol m^{-2} s^{-1}), and A_X is the surface area of the solid (m^2). This leads to the following expression,

$$dF_X = r_X dA_X. \quad \text{(A3)}$$

Due to a changing amount of solid available for reaction, the molal flow rate at any point in time, F_X, can be expressed in terms of the original molal flow rate, F_{X0}, and f_X, the fractional amount of mineral dissolved, such that

$$F_X = F_{X0}(1 - f_X). \quad \text{(A4)}$$

Combining Eqns. A3 and A4 results in

$$\frac{dA_X}{F_{X0}} = \frac{df_X}{(-r_X)}. \quad \text{(A5)}$$

Equation A5 can be integrated over the entire reactor to give

$$\frac{A_X}{F_{X0}} = \int_{f_{X_{in}}}^{f_{X_{out}}} \frac{df_X}{(-r_X)}. \quad \text{(A6)}$$

Since F_X can also be expressed as the product of the concentration C_X and the flow rate ϑ_0, one can write that $F_X = C_X \cdot \vartheta_0$; upon substitution of this product into Eqn. A4, Eqn. A6 can be rewritten in the following manner,

$$\frac{A_X}{\vartheta_0} = \int_{C_{X_{in}}}^{C_{X_{out}}} \frac{dC_X}{(r_X)}. \quad \text{(A7)}$$

The solution to the above equation depends on the type of reactor. Restricting ourselves to well-mixed (CSTR) and tubular reactors; in the former case, the overall rate of dissolution r (from r_X/δ_X, where δ_X is the formula stoichiometric coefficient for species X) is the same everywhere in the reactor, and, therefore, it can be treated as a constant and taken outside of the integral. This allows for a straightforward solution to Eqn. A7,

$$r = \frac{(C_{X_{out}} - C_{X_{In}})\vartheta_0}{\delta_X A_X}. \quad \text{(A8)}$$

On the other hand, in a tubular reactor, where reaction takes place along the entire length of the reactor, the reaction rate r varies as a function of position in the reactor (due to changing chemical affinity, pH, etc.). In this case, r is not a constant, and the solution of Eqn. A7 is not straightforward.

However, in some cases, the experimental design and operating conditions allow for the reaction rate r to be treated as a constant in a tubular reactor. For this study, the tubular reactor was treated as a well-mixed reactor due to the valid approximation that there was no change (gradient) in the reaction rate as a function of reactor length. This can be attributed to the following reasons:

1. small size of sample with respect to overall reactor length;
2. slow dissolution kinetics of mineral; and
3. high flow rates and turbulent flow around the sample (high Reynolds number).

The three reasons above, when taken together, imply that when a fluid packet passes over the mineral sample, the entire mineral surface has the same intrinsic rate of reaction with the solution. This is quite logical, given the fact that the contact time of an individual packet of fluid with the mineral is extremely short. For this reason, there is no significant development of a pH or concentration (chemical affinity) gradient around the sample. One must note, however, that the lack of a concentration gradient doesn't mean that the mineral doesn't react; what is implied is that the hydrodynamics of turbulent flow (on a microscale) around a sufficiently small sample ensure that the mineral surface, on average, is in contact with a solution of uniform pH and chemical affinity. For this reason, a tubular reactor containing a single sample of a sparingly soluble mineral satisfies the conditions of a uniform reaction rate, and the well-mixed reactor rate extrapolation (Eqn. A8) can be safely applied.

Obviously, the above would not be true if a tubular reactor were packed with mineral grains. In such a case, the reaction rate of a certain grain would be dependent on its axial position within the reactor. This is due to the fact that the chemistry of the solution is continuously changing as it flows downstream through the reactor. Thus, at a certain location in the reactor, a given packet of fluid has a solution chemistry determined by reactions with all of the grains lying upstream and having already reacted with this given packet of fluid. For this reason, the reaction rate should decrease as a function of axial length. The extrapolation of an overall rate of reaction under such conditions generally requires the use of reactor performance equations that explicitly take into account the nonuniformity of the reaction rate.

Table A1. Comparison of quartz dissolution rates at 300°C in deionized water. The similarity in rates is used to justify the derived expression for the mixed-flow reactor rate equation (see text for details).

reference	material and dimensions	remarks on rate det'n.	log rate (mol m^{-2} s^{-1})
this study:	single slab	mass loss	-6.63
(tubular reactor)	1.0 x 0.8 x 0.2 (cm)	$[Si]_{aq}$	-6.66
DOVE and	grains		
CRERAR, 1990	150-250 μm ø	$[Si]_{aq}$	-6.27
(mixed-flow reactor)		"	-6.31
		"	-6.45
RIMSTIDT and	grains	$[Si]_{aq}$	-7.25
BARNES, 1980	125-1000 μm ø	(regression)	
(batch reactor)			

The validity of the well-mixed reactor assumption was tested by the determination of the rate of dissolution of quartz in deionized water at 300°C. A quartz slab was hydrolyzed over a period of 17 days in the same tubular reactor used for the albite study, and the dissolution kinetics were measured both in terms of mass loss and the steady state aqueous concentration of released Si. The rates that were obtained using the well-mixed reactor rate equation (Eqn. A8) were within 0.1 to 0.4 log units (mol m^{-2} s^{-1}) of the values reported by DOVE and CRERAR (1990) for the kinetics of quartz dissolution under the same conditions using a well-mixed flow reactor (see Table A1 for results). It is interesting to note that the results from this study and those from DOVE and CRERAR (1990) are considerably higher than the dissolution rates obtained using a static reactor in the study of RIMSTIDT and BARNES (1980)—(the rates are compared in Table A1). This difference in rates may be an example of how the experimental design can influence the measured reaction rates. The differences are most probably attributable to the higher chemical affinities attainable in flow reactors. In addition, flow reactors are more amenable to the measurement of reaction rates which are not limited by the diffusion of reaction products away from the liquid-solid interface.

In conclusion, one must note that there is no single cutoff criterion that can be used to describe the transition from one flow reactor type to another. The application of well-mixed reactor rate theory works well when a single crystal sample is hydrolyzed under conditions utilizing a sufficiently high flow rate (no attempt is made to define a flow rate limit). On the other hand, a tubular reactor that is packed with a crushed mineral sample over its entire length would probably not be an ideal case for applying the well-mixed reactor assumption. Nonetheless, each case requires verification, as was done in this case. In general, the exact quantification of reactor behavior is dependent on many variables and cannot be discussed in detail here; however, reactor modeling is treated extensively in the chemical engineering literature.